Asian Journal of Chemistry; Vol. 27, No. 12 (2015), 4541-4548

ASIAN JOURNAL OF CHEMISTRY

http://dx.doi.org/10.14233/ajchem.2015.19219

Modeling Ultrasound-Assisted Decolorization Efficiency of Reactive Red 195 Using Soybean Cake

MUSA BUYUKADA and FATIH EVRENDILEK*

Department of Environmental Engineering, Abant Izzet Baysal University, Bolu, Turkey

*Corresponding author: E-mail: fevrendilek@ibu.edu.tr

Received: 31 March 2015; *Accepted*: 18 May 2015; *Published online*: 29 August 2015; AJC-17505

Soybean cake was utilized as an adsorbent for the decolorization of Reactive Red 195 from aqueous solution based on adsorption, ultrasound and ultrasound-assisted adsorption. This study quantified and modeled effects of the following six factors on decolorization efficiency: the three process types, five initial dyestuff concentrations, five initial pH values, four adsorbent concentrations, four temperatures and 16 reaction times. Optimum pH for adsorption was determined as 2. The maximum decolorization efficiency (93.3 %) was obtained consistently with ultrasound-assisted adsorption, the lowest initial dye concentration (200 mg/L), the highest adsorbent concentration (2 g/L) and the highest temperature (50 °C). The best-fit multiple non-linear regression models accounted for 85.1 to 93.3 % of variation in decolorization efficiency, had a cross-validation-derived predictive power that ranges from 84.2 to 92.8 % and quantified the rates of change in decolorization efficiency as a function of the experimental predictors. Pseudo-second-order kinetic model described decolorization kinetics of Reactive Red 195 better than pseudo-first-order kinetic model. The Langmuir adsorption model fitted the adsorption equilibrium data better than the Freundlich model. The adsorption of Reactive Red 195 on soybean cake was found to be of endothermic and spontaneous nature.

Keywords: Color removal, Isotherms, Kinetics, Data-driven modeling, Soybean cake.

INTRODUCTION

Synthetic dyestuffs widespread in textile, paper printing, food, cosmetics, pharmaceutics industries and color photography are of great concern as important environmental pollutants to well-being of humans and ecosystems since there are more than 10000 commercially available dyes most of which are difficult to biodegrade due to their complex aromatic molecular structure and synthetic origin[1-3]. Therefore, an effective process for the removal of dyes before their disposal as wastewaters is of environmentally and economically great importance[4]. Traditional treatment methods to achieve decolorization of such wastewaters include chemical coagulation and/or ozonation[5,6], electrochemical treatment[7,8] and biological treatment[9]. However, these common treatment methods are often ineffective in decolorizing of dyes which are formed from highly complex and variable chemical structures[2,10]. Adsorption technique has been showed to be an effective process for the removal of color from dye wastewaters as well as for the treatment of industrial wastewaters owing to its efficiency, flexibility and economic feasibility[11-13].

Numerous kinds of adsorbents such as (dehydrated) wheat bran carbon[10], (dehydrated) peanut hull[3,12], chemically treated tomato waste[14], natural bentonite[15], chitosan[16] and dead pine needles[13] have been used in the decolorization process. Recently, the use of adsorbents of vegetable origin has gained increasing importance through which non-toxic by-products and wastes are used as an ecologically benign alternative in decolorization of textile dyes. Soybean cake as a by-product of oil industry is generally used as a domestic animal feed and to our best knowledge, has not been explored as an adsorbent for reactive dyestuffs.

Nowadays, advanced oxidation processes such as ozone oxidation, ultrasound irradiation, photocatalytic degradation and electro-Fenton process have also gained importance in a wide variety of application fields, especially, in the treatment and decolorization of dye solutions from wastewaters[17,18]. There exists recently increased interest in the applications of sono-chemical treatments to wastewaters contaminated with dyes, aromatic compounds and/or chlorinated hydrocarbons[19-22]. Ultrasound causes the formation, growth and sudden collapse of acoustic cavitation-induced micro bubbles in an irradiated liquid leading to high localized temperatures (up to 5000 °C) and pressures (hundreds of bars)[23-25]. Although most organic compounds can be decomposed by the ultrasonic irradiation, much effort has been devoted to accelerate the decomposition rates that are still slow for practical uses[15].

In present study, decolorization efficiency by soybean cake of dyestuff aqueous solutions of Reactive Red 195 (RR195) using adsorption, ultrasound and ultrasound-assisted adsorption was quantified as a function of process type, dye concentration, adsorbent concentration, temperature and reaction time.

EXPERIMENTAL

Soybean cake was used in the present study as an adsorbent and was supplied from a local oil firm in Ordu, Turkey. Soybean cake was sieved using American Society for Testing and Materials (ASTM) standard sieves (E-872 and D-1102) after being grinded using a ball mill (Mertest LB 220). In all the experiments, soybean cakes sieved to 50-100 mesh size were used without any other treatment. Surface area and porosity of soybean cake were measured using a BET analyzer (ASAP 2020, Micnometrics Inc., USA) based on liquid N_2 adsorption onto adsorbent at 77 K. Prior to BET analyses, soybean cake was subjected to pre-treatment of degassing at 1.3×10^{-2} Pa for 6 h. Surface area of soybean cake was measured at 2.08 m^2/g. Porosity of soybean cake was measured determining the total amount of adsorbent held at a relative pressure of 0.95. Results showed that soybean cake had a fairly porous structure. Chemical properties of soybean cake was determined using a FTIR spectroscopy (ATI Unicam Mattson 1000) (Fig. 1). After soybean cake was mixed with KBr with a mass ratio of 1:33, the mixture was treated under a hydraulic pressure of 490.3 MPa for two minutes in order for all the samples to become pellets. Pellets of 1 mm in thickness were dried in an oven (DV452, Chanel, China) for 2 h. Zero point charge (pH_{zpc}) of soybean cake and isoelectric point (pH_{iep}) of Reactive Red 195 were also measured using a zeta potential meter (Zetasizer, 3000HSA, Malvern, UK) and a titration method, respectively, according to Dincer *et al.*[5].

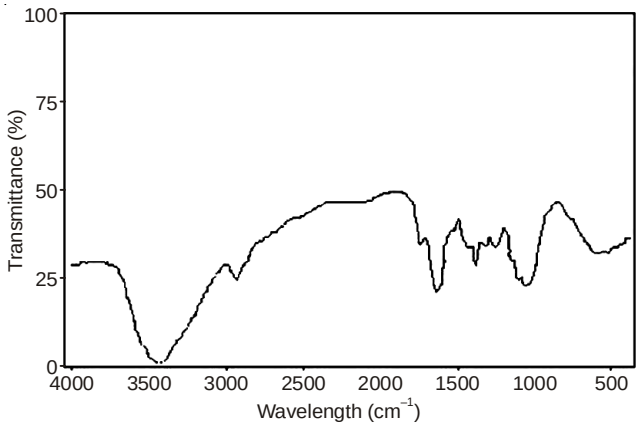

Fig. 1. FTIR spectroscopy of soybean cake

The commercial azo dye with the Color Index generic name of Reactive Red 195 (RR195; $C_{31}H_{19}ClN_7O_{19}S_6Na_5$; molecular weight = 1136.31 g/mol; λ_{max} = 540) was obtained from a local textile firm in Duzce (Turkey) and was used without further purification. The stock solutions of Reactive Red 195 were prepared in a constant concentration of 1.0 g/L and then diluted to appropriate concentrations. Working solutions of the desired concentrations were obtained using successive dilutions. The initial pH of each solution was adjusted to the required value with concentrated and diluted H_2SO_4 and NaOH solutions before mixing the soybean cake.

Batch sorption experiments were carried out following the experimental set-up shown in Fig. 2. The experiments were performed in a 1000 mL cylindrical jacketed vessel put on an overhead mechanical stirrer (IKA RW 20, Kutay Group, Turkey) which stirred the mixture at an agitation speed of 400 rpm. The agitator was used to have well-mixed suspension characteristics for the solid particles. The vessel was set in a digital ultrasonic cleaner (Wise Clean WUC D06H, Wisd Laboratory, Germany) operating at a frequency of 40 kHz. Soybean cake concentration of 1 g/L was contacted with Reactive Red 195 solution of 500 mL for the decolorization of aqueous dye solutions. The experiments were repeated for the three process types of adsorption, ultrasound and ultrasound-assisted adsorption, the five initial pH values of 1, 1.5, 2, 2.5 and 3, the five initial dye concentrations of 200, 225, 250, 275 and 325 mg/L, the four adsorbent concentrations of 0.5, 0.75, 1.0 and 2.0 g/L, the four temperatures of 20, 30, 40 and 50 °C and the 16 reaction times of 0, 5, 10, 15, 20, 25, 30, 45, 60, 75, 90, 120, 150, 180, 210 and 240 min. Ultrasound power used for the treatments was 510 W.

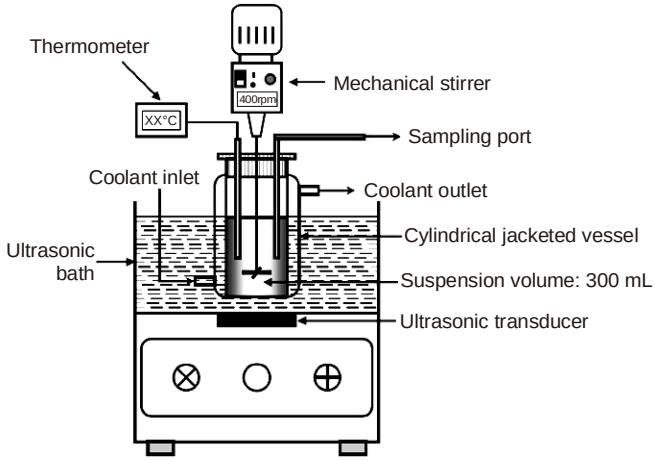

Fig. 2. Schematic view of the experimental set-up used in the present study

The solutions were analyzed at predetermined time intervals for the final concentration of Reactive Red 195 using a UV/visible spectrophotometer (Shimadzu UV-2100, Biomerieux, France) at a wave length of 540 nm for the maximum absorbance value. Dye concentration was calculated from a calibration curve. Decolorization efficiency (DE, %) at any time was estimated as follows[2,3]:

$$DE = \frac{A_o - A_t}{A_o} \times 100 \quad (1)$$

where A_o and A_t are the initial and measured absorbance values of the samples at a specified interval during a 4 h reaction, respectively. Dyestuff concentration (C_{RR195}, mg/L) after each experiment was calculated using the best-fit calibration graph (absorbance = $0.0189 \times C_{RR195}$; $R^2 = 0.99$; $p < 0.001$).

Reaction kinetics parameters (rate and order of reaction rate) of the three process types were derived from the experimental data and were used to estimate activation energy of

reaction for the processes. Langmuir and Freundlich isotherm studies were performed under pH 2, the initial dye concentration range of 200 to 500 mg/L, the 4 h reaction time and the temperature range of 20 to 50 °C. Finally, enthalpy, Gibbs free energy change and entropy were determined using isotherm constants.

Decolorization efficiency was tested as a function of (1) the initial dye concentrations, the process types and the reaction times under the constant adsorbent concentration (1 g/L) and temperature (20 °C); (2) the adsorbent concentrations, the process types and the reaction times under the constant dye concentration (250 mg/L) and temperature (20 °C) and (3) temperature, the process types and reaction time under the constant dye (250 mg/L) and adsorbent (1.0 g/L) concentrations. Anderson-Darling test and the plots of both residuals *versus* fitted values and residuals *versus* the order of the data were applied to check the assumptions of normality, constant variance and autocorrelation, respectively, prior to the implementation of the parametric tests of analysis of variance (ANOVA) and multiple non-linear regression (MNLR). Tukey's multiple comparisons following general linear model (GLM) was used to detect significant differences in decolorization efficiency among the three processes, the reaction times, the initial dye concentrations, the adsorbent concentrations and the temperatures. Best-fit MNLR models were built to explicate the efficacy of explanatory factors and their interactions for the prediction of the response variable (decolorization efficiency). The best subset procedure was used to choose the best-fit MNLR models with the highest goodness-of-fit and the highest predictive power which were measured by adjusted coefficient of determination (R^2_{adj}) and coefficient of determination based on leave-one-out cross-validation (R^2_{CV}). The three-category process type was incorporated in the MNLR models as a dummy variable with ultrasound-assisted adsorption held as baseline. Variance inflation factor (VIF) for multicollinearity and Durbin-Watson (D-W) statistics for autocorrelation were reported for the best-fit MNLR models. All the statistical analyses were performed using Minitab 16.1 (Minitab, Inc., State Collage, PA).

RESULTS AND DISCUSSION

Descriptive statistics of decolorization of Reactive Red 195 were presented as a function of process type, temperature, reaction time, initial dye concentration, adsorbent concentration and reaction time in Table-1. Out of the five pH values, the minimum decolorization efficiency was obtained at the initial pH 3 for the aqueous reactive dyestuff solution under the treatment of 250 mg/L Reactive Red 195 with 1.0 g/L soybean cake at 20 °C and the agitation speed of 400 rpm. Decolorization efficiency increased with a decreasing pH ($p < 0.05$; $n = 75$) and reached its maximum at the lowest pH 1 as the reaction time progressed (Fig. 3). Effect of initial pH on decolorization efficiency depends on pH_{zpc} of adsorbent and pH_{IEP} of dye stuff[5]. pH_{zpc} of soybean cake and pH_{IEP} of Reactive Red 195 were measured at 1.5 and 2.5, respectively. The dyestuff gets negatively charged with pH values above 2.5, thus serving as a repulsive force between the dye and the negatively charged adsorbent. Decolorization efficiency was reported to increase when the

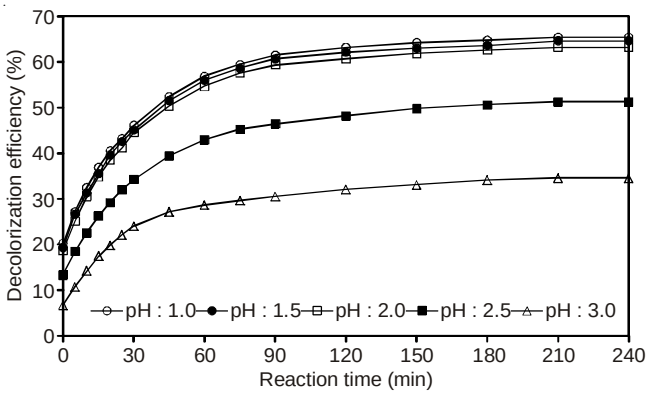

Fig. 3. Effect of initial pH on decolorization by soybean cake of Reactive Red 195 using adsorption (Total mixture volume of 500 mL; total reaction time of 4 h; 250 mg/L initial Reactive Red 195 concentration; and 1.0 g/L soybean cake concentration)

initial pH of reactive dye solution was set in a range of 1.5 to 2.5 which was attributed to the strongly electrostatic attraction force between adsorbent and dyestuff[26]. Similarly, an increase in adsorption capacity was stated with increasing pH up to pH 9[5]. Therefore, pH 2 was assumed to be the optimum pH value for the decolorization experiments conducted in the present study.

Tukey's multiple comparison test showed that the three process types and the five initial dye concentrations differed significantly from one another in terms of decolorization efficiency ($p < 0.001$) (Table-2). The highest decolorization efficiency of 65.9 % was obtained at the lowest initial dye concentration of 200 mg/L with ultrasound-assisted adsorption. Similarly, decolorization efficiency was found to decrease with the increasing initial dye concentration in the decolorization of methyl orange with ultrasonic irradiation-assisted ozonation[27]. The reaction times of 0, 5, 10, 20, 45 and 150 min differed significantly in generating an increased efficiency of decolorization in the present study. Ultrasound-assisted adsorption yielded the highest decolorization efficiency of 47.2 % in the first 10 min, a reaction time shorter than did the other process types.

The best-fit MNLR model accounted for 89 % of variation in decolorization efficiency and had a high predictive power (R^2_{CV} = 89 %) based on cross-validation as a function of the process type, reaction time, initial dye concentration, an interaction term among adsorption, reaction time and initial dye concentration and the quadratic and cubic terms of reaction time ($p < 0.001$) (Table-3). The increased initial dye concentration decreased decolorization efficiency at a rate of 0.1 mg/L, whereas the increased reaction time increased decolorization efficiency at a rate of 0.7 min^{-1}. As with our findings, both an inverse relationship between initial dye concentration and decolorization efficiency and a positive relationship between adsorbent concentration and decolori-zation efficiency were found based on the best-fit MNLR models for the decolorization of Reactive Blue 19 from aqueous solution with a combined ultrasound/activated carbon system and for the adsorption of Reactive Black 5 in aqueous solution by peanut hull, respectively[1,3]. Relative to ultrasound-assisted adsorption, adsorption and ultrasound separately led to decolorization efficiency lower by 21 % and 4 %, respectively. Using the best-fit MNLR models, Sayan and Esraedecan[1] also detected the same positive

TABLE-1
DESCRIPTIVE STATISTICS OF DECOLORIZATION EFFICIENCY (%) OF REACTIVE RED 195 BY SOYBEAN CAKE ACCORDING TO PROCESS TYPE, TEMPERATURE, REACTION TIME, INITIAL DYE CONCENTRATION and ADSORBENT CONCENTRATION

Factor	n	Mean	SE	Mode	Median	Skewness	Kurtosis
Process type							
Adsorption	176	50.8	15.6	52.7	64.5	-0.62	-0.45
Ultrasound	176	62.0	13.4	66.6	63.3	-1.32	1.55
Ultrasound-assisted adsorption	176	66.3	13.4	70.4	62.8	-1.19	1.18
Temperature (°C)							
20	384	56.5	15.5	59.9	73.6	-0.84	0.12
30	48	63.5	12.4	68.3	48.4	-1.53	1.49
40	48	68.4	11.6	72.5	47.1	-1.57	1.81
50	48	72.5	11.3	76.6	46.7	-1.49	1.69
Initial dye concentration (mg/L)							
200	48	65.8	11.6	69.5	49.0	-1.64	2.13
225	48	61.4	13.5	66.6	52.0	-1.46	1.18
250	336	61.5	15.5	66.4	71.4	-0.92	0.24
275	48	53.1	14.2	58.3	53.8	-1.22	0.53
325	48	46.0	14.0	51.3	51.5	-1.19	0.34
Adsorbent concentration (g/L)							
0.5	48	61.9	19.2	70	70.4	-1.18	0.31
0.75	48	59.9	15.9	65.9	59.7	-1.39	0.93
1	384	61.0	15.1	65.4	74.6	-1.08	0.7
2	48	46.6	7.2	49.6	30.5	-2.85	7.56
Reaction time (min)							
0	33	27.7	10.6	26.7	43.3	0.51	-0.37
5	33	43.8	14.5	43.6	56.1	-0.08	-0.62
10	33	51.1	15.1	52.8	57.9	-0.37	-0.66
15	33	55.0	14.7	57.4	57.4	-0.42	-0.69
20	33	57.5	14.0	60.1	55.1	-0.41	-0.72
25	33	59.3	13.2	61.7	52.0	-0.38	-0.77
30	33	60.8	12.4	63.1	49.1	-0.34	-0.82
45	33	63.2	10.9	64.7	43.1	-0.32	-0.82
60	33	64.7	10.1	65.5	39.3	-0.33	-0.76
75	33	65.6	9.6	67.1	36.1	-0.36	-0.72
90	33	66.2	9.3	68.1	34.5	-0.41	-0.61
120	33	67.0	9.2	69.4	33.7	-0.5	-0.44
150	33	67.7	9.1	69.8	33.5	-0.58	-0.31
180	33	68.1	9.1	70.4	33.7	-0.64	-0.23
210	33	68.5	9.2	70.8	33.8	-0.68	-0.17
240	33	68.6	9.2	71.2	33.8	-0.68	-0.15

relationship between decolorization efficiency and the interaction term between initial dye concentration and reaction time in present study.

According to Tukey's multiple comparisons, the ultrasound-assisted adsorption resulted in the highest decolorization efficiency of 93.3 % with the highest adsorbent concentration (2 g/L) ($p < 0.001$) (Table-2). Decolorization efficiency increased significantly with the reaction times of 0, 5, 10, 25 and 150 min. The best-fit MNLR model explained 93 % of variation in decolorization efficiency with a high predictive power (R^2_{CV} = 92 %) as a function of the process type, the adsorption concentration, the reaction time, an interaction term between adsorption and reaction time and the quadratic and cubic terms of the reaction time (Table-3). An increase in the adsorbent concentration or the reaction time enhanced decolorization efficiency at a rate of 40.4 g/L and 0.7 min^{-1}, respectively. Ultrasound-assisted adsorption yielded decolorization efficiency better than adsorption by 17 % and ultrasound by 3 %. Ultrasound-assisted adsorption was faster than the other processes in paving the way for the highest decolorization efficiency with the increasing adsorbent concentration as well as the increasing reaction time, respectively. In present study, the same positive relationship was found between reaction time and decolorization efficiency based on the best-fit MNLR models[1,17,28].

Based on Tukey's multiple comparisons, decolorization efficiency was significantly higher with the ultrasound-assisted adsorption process and with the increasing temperature ($p < 0.001$) (Table-2). The highest decolorization efficiency of 72.6 % at 50 °C and 58.3 % in the initial 10 min was achieved more rapidly with ultrasound-assisted adsorption than the other process in the face of the increasing temperature and the increasing reaction time, respectively. 94 % decolorization efficiency was obtained based on the adsorption of Chemazol Reactive Red 195 on dehydrated beet pulp carbon with a 20 mg/L initial dye concentration at 50 °C[29]. 98.6 % decolorization efficiency was reported for the triphenylmethane dyes wastewater using ultrasonic-assisted ozone oxidation under the optimal conditions of 39.8 °C and initial pH 5.2[17,18]. The optimal decolorization efficiency of Reactive Red 2 was estimated at 85 % after a 120 min reaction time at pH 7 using an ultraviolet/ultrasound/TiO_2 system[30].

TABLE-2
TUKEY'S MULTIPLE COMPARISONS OF DECOLORIZATION EFFICIENCY (%) AMONG PROCESS TYPES, INITIAL DYE CONCENTRATIONS, REACTION TIMES, TEMPERATURES AND ADSORBENT CONCENTRATIONS ($p < 0.001$)

	Mean	Mean	Mean
Process type	n = 80	n = 64	n = 64
Adsorption	47.6[a]	49.5[a]	56.5[a]
Ultrasound	59.1[b]	58.7[b]	67.9[b]
UAA	63.6[c]	61.8[c]	72.1[c]
Reaction time (min)	n = 15	n = 12	n = 12
0	25.2[i]	23.5[g]	35.5[h]
5	40.0[h]	42.6[f]	51.3[g]
10	47.2[g]	49.7[e]	58.3[f]
15	51.2[fg]	53.3[de]	61.7[ef]
20	53.9[ef]	55.3[cde]	63.8[de]
25	55.9[def]	56.8[bcd]	65.4[cde]
30	57.5[cde]	58.0[abcd]	66.6[bcde]
45	60.3[bcd]	60.2[abc]	68.7[abcd]
60	62.0[abc]	61.5[abc]	70.1[abc]
75	63.1[ab]	62.2[ab]	70.9[ab]
90	63.8[ab]	62.7[ab]	71.4[ab]
120	64.7[ab]	63.4[ab]	72.0[a]
150	65.4[a]	64.0[a]	72.5[a]
180	65.8[a]	64.3[a]	73.0[a]
210	66.2[a]	64.6[a]	73.4[a]
240	66.3[a]	64.7[a]	73.4[a]

Initial dye conc. (mg/L)	Mean (n = 48)	Adsorbent conc. (g/L)	Mean (n = 48)	Temp. (°C)	Mean (n = 48)
200	65.9[a]	0.50	31.0[a]	20	57.5[a]
225	61.4[b]	0.75	45.0[b]	30	63.5[b]
250	57.5[c]	1.00	57.5[c]	40	68.4[c]
275	53.1[d]	2.00	93.3[d]	50	72.6[d]
325	46.0[e]	–	–	–	–

UAA = Ultrasound-assisted adsorption. Means that do not share the same letter are significantly different at $p < 0.001$.

TABLE-3
BEST-FIT MNLR MODELS OF DECOLORIZATION EFFICIENCY (%) UNDER CONSTANT CONDITIONS OF (1) 20 °C AND ADSORBENT CONCENTRATION OF 1 g/L; (2) 20 °C AND INITIAL DYE CONCENTRATION OF 250 mg/L; AND (3) INITIAL DYE CONCENTRATION OF 250 mg/L AND ADSORBENT CONCENTRATION OF 1 g/L ($p < 0.001$)

Explanatory variables	(1)	(2)	(3)	VIF
Intercept	87.837	-2.179	39.553	
Adsorption	-21.53	-17.463	-19.387	2
Ultrasound	-4.518	-3.075	-4.247	1
RT (min)	0.723	0.718	0.658	70
IDC (mg/L)	-0.165			1
AC (g/L)		40.431		1
T (°C)			0.466	1
Adsorption × RT × IDC	0.0002			2
Adsorption × RT		0.064		2
Adsorption × RT × T			0.001	2
RT^2	-0.005	-0.005	-0.005	428
RT^3	0.000013	0.000013	0.000012	177
R^2_{adj} (%)	89.6	93.3	85.1	
R^2_{CV} (%)	89.2	92.8	84.2	
SE (%)	4.85	6.84	5.23	
D-W	0.99	1.26	0.93	
n	240	192	192	

AC = Adsorbent concentration; D-W = Durbin-Watson statistics; IDC = Initial dye concentration; RT = Reaction time; VIF = Variation inflation factor.

In the present study, the reaction times of 0, 5, 10, 20 and 60 min led to significantly increased decolorization efficiency (Table-2). Consistent with our findings, decolorization efficiency was reported to increase with the increasing temperature reaching 93 % at 40 °C and with increasing reaction time reaching 85 % in the first 10 min as a result of ultrasound-assisted Fenton oxidation in the treatment of ammunition wastewater[22]. The best-fit MNLR model elucidated 85 % of variation in decolorization efficiency with R^2_{CV} = 84 % as a function of process type, temperature, reaction time, a three-way interaction term among adsorption, reaction time and temperature and the quadratic and cubic terms of reaction time (Table-3). The rate of change in decolorization efficiency was estimated at 0.4 °C and 0.6 min^{-1}. Ultrasound-assisted adsorption performed decolorization efficiency better than adsorption by 19 % and ultrasound by 4 % (Table-3). Sayan and Esraedecan[1] pointed out to the same positive correlation between temperature and decolorization efficiency, while Zhou *et al.*[17,18] modeled the same positive correlation between decolorization efficiency and the temperature × reaction time interaction based on the best-fit MNLR models.

Pseudo-first-order and second-order kinetic models are the most common ones to describe decolorization kinetics[5,31]. Our results showed that pseudo-second-order kinetic model described decolorization kinetics of Reactive Red 195 better than pseudo-first-order kinetic model (Table-4) and was calculated as follows[5,31]:

$$\frac{dq_t}{dt} = k_2(q_e - q_t)^2 \quad (2)$$

The integration of eqn. 2 at the boundary condition provides the following eqn. 3:

$$\frac{1}{(q_e - q_t)} = \frac{1}{q_e} + k_2 t \quad (3)$$

The rearrangement of eqn. 3 generates the below equation:

$$\frac{t}{q_t} = \frac{1}{k_2 q_e^2} + \frac{t}{q_e} \quad (4)$$

where k_2 is the rate constant of pseudo-second-order reaction (g/mg/min), q_e is the amount of dye removed at equilibrium (mg/g), q_t is the amount of dye removed at time t (mg/g). Our results are in agreement with findings reported by Al-Ghouti[32] and Ozacar and Sengil[33]. Also, the increased second-order rate constant with the increasing temperature indicated that all the decolorization processes in the present study were endothermic. The activation energy (E_A) estimates of the decolorization processes decreased in the order of adsorption > ultrasound > ultrasound-assisted adsorption (Table-4).

Isotherms were used to determine the amount of adsorbent required to remove one unit mass of dyestuff and adsorption capacity. The following Langmuir and Freundlich isotherm models as eqns. 5 and 6, respectively, were fitted into the experimental data[5,10,29]:

$$\frac{C_e}{q_e} = \frac{1}{q_{max} K_L} + \frac{1}{q_{max} C_e} \quad (5)$$

where q_e is the amount of adsorbed dye (mg/g), C_e is the equilibrium liquid-phase concentration (mg/L), K_L is a direct measure of sorption intensity (L/mg) and q_{max} is a constant

TABLE-4
PSEUDO-FIRST-ORDER AND PSEUDO-SECOND-ORDER KINETIC MODELS OF ADSORPTION, ULTRASOUND AND ULTRASOUND-ASSISTED ADSORPTION PROCESSES

Temp. (°C)	Pseudo-first-order				Pseudo-second-order			
	q_e (mg/g)	$q_{e,det}$ (mg/g)	k_1 ($\times 10^3$) (min^{-1})	R^2	$q_{e,det}$ (mg/g)	k_2 ($\times 10^4$) (g/mg/min)	R^2	E_A (J/mol)
Adsorption								
20	158.0	99.17	23.53	0.994	165.8	5.30	0.998	22.32
30	171.0	79.60	20.59	0.964	175.8	7.30	0.999	
40	178.5	70.00	22.45	0.971	181.8	9.86	0.999	
50	184.3	64.06	25.17	0.963	187.3	12.32	0.999	
Ultrasound								
20	168.1	37.23	24.32	0.841	169.2	25.33	0.999	18.06
30	180.5	28.20	21.53	0.779	181.2	33.26	0.999	
40	189.9	20.84	19.07	0.693	190.5	43.13	0.999	
50	198.0	17.85	18.45	0.678	198.4	49.81	0.999	
Ultrasound-assisted adsorption								
20	178.8	33.62	23.48	0.818	179.9	28.36	0.999	17.29
30	188.0	24.68	20.43	0.767	188.7	36.82	0.999	
40	198.5	20.14	20.91	0.726	199.2	46.84	0.999	
50	209.6	18.79	22.85	0.756	210.1	54.33	0.999	

related to adsorbent monolayer reflecting the maximum adsorption capacity (mg/g).

$$\log q_e = \log K_f + \frac{1}{n}\log C_e \quad (6)$$

where q_e is the amount of dye adsorbed per unit mass of adsorbent (mg/g), C_e is the equilibrium concentration of dye in solution (mg/L) and K_f and n are Freundlich constants.

As shown in in Fig. 4, Langmuir adsorption model fitted the experimental data better than did the Freundlich model (Table-5), as was also found by Gong *et al.*[34]. A dimensionless separation constant of equilibrium (R_L) was calculated for all the processes. R_L was used to express the shape of Langmuir isotherm and thus, applicability of decolorization process as follows[35]:

$$R_L = \frac{1}{1 + K_L C_o} \quad (7)$$

where K_L is the constant of Langmuir isotherm and C_o is initial dye concentration adsorbed. According to eqn. 7: process is unrealizable if $R_L > 1$; shape of isotherm is linear if $R_L = 1$; process is realizable if $0 < R_L < 1$ and process is irreversible if $R_L = 0$. In the present study, all the R_L values were found to vary between 0 and 1 which showed that all the decolorization processes were realizable.

Gibbs free energy and entropy are the most common thermodynamic parameters for the identification of a decolorization process. An increase in entropy is an indicator of the structural heterogeneity of dyestuff according to the second and third laws of thermodynamics[36]. Gibbs free energy as a function of entropy and temperature provides information about spontaneity of a chemical reaction[37]. Gibbs free energy and entropy can be calculated as follows[10]:

$$\Delta G = \Delta H - T\Delta S = -RT \ln K \quad (8)$$

By rearranging eqn. 8, eqn. 9 was derived thus:

$$\ln K = \frac{\Delta S}{R} - \frac{\Delta H}{R}\frac{1}{T} \quad (9)$$

TABLE-5
LANGMUIR AND FREUNDLICH ISOTHERM CONSTANTS OF ADSORPTION, ULTRASOUND AND ULTRASOUND-ASSISTED ADSORPTION PROCESSES

Temp. (°C)	Langmuir isotherm				Freundlich isotherm		
	q_{max} (mg/g)	K_L (L/mg)	R_L	R^2	K_f	n	R^2
Adsorption							
20	206.6	0.0322	0.111	0.999	75.96	6.258	0.987
30	216.0	0.0395	0.092	0.998	88.93	6.978	0.941
40	223.7	0.0439	0.084	0.998	94.32	7.062	0.945
50	229.9	0.0491	0.075	0.999	102.1	7.468	0.959
Ultrasound							
20	226.2	0.0326	0.112	0.998	79.03	5.893	0.985
30	238.1	0.0404	0.094	0.999	91.86	6.390	0.972
40	250.6	0.0462	0.085	0.998	102.8	6.770	0.991
50	263.2	0.0528	0.077	0.997	112.4	6.998	0.981
Ultrasound-assisted adsorption							
20	248.1	0.0332	0.114	0.998	81.61	5.488	0.983
30	257.1	0.0413	0.102	0.997	96.15	6.131	0.988
40	266.7	0.0479	0.087	0.996	109.3	6.716	0.981
50	274.0	0.0545	0.078	0.992	126.2	7.837	0.969

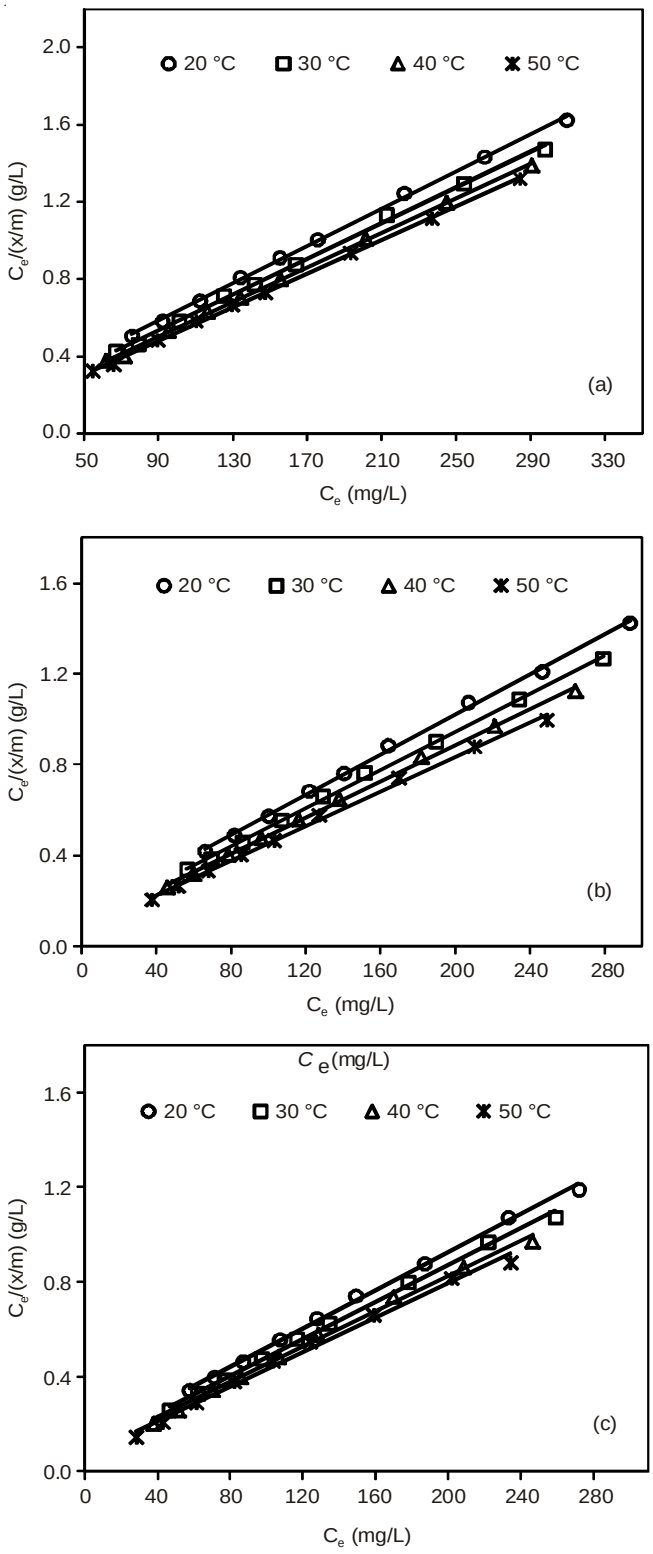

Fig. 4. Langmuir isotherm plots for (a) adsorption, (b) ultrasound and (c) ultrasound-assisted adsorption

where ΔG is Gibbs free energy (kJ/mol), ΔH is enthalpy of reaction (kJ/mol), K is chemical equilibrium (Langmuir) constant (L/mol) and T is temperature (K). When ln K *versus* 1/T graph is plotted, the slope and intercept of the plot can be used to determine enthalpy and entropy of the reaction, respectively. Results showed that all processes had a positive enthalpy and were endothermic and spontaneous in nature (Table-6). The fact that Gibbs free energy changes were negative for all the temperatures showed that the process was of endothermic and spontaneous nature in the present study (Table-6). The increase in entropy depending on the process type indicates increased structural heterogeneity of the dyestuff. Changes in entropy were determined for all the temperatures and the processes (Table-6). Positive change in entropy can be attributed to high affinity of the adsorbent to the dyestuff which was also indicated by Mittal[38].

TABLE-6
THERMODYNAMIC CONSTANTS OF ADSORPTION, ULTRASOUND AND ULTRASOUND-ASSISTED ADSORPTION PROCESSES

Temp. (°C)	K (L/mg)	ΔG (kJ/mol)	ΔS (kJ/mol/K)	ΔH (kJ/mol)
Adsorption				
20	0.0321	-25.59	0.1244	10.86
30	0.0395	-26.98	0.1249	
40	0.0439	-28.15	0.1246	
50	0.0490	-29.34	0.1244	
Ultrasound				
20	0.0325	-25.62	0.1301	12.50
30	0.0404	-27.04	0.1305	
40	0.0461	-28.28	0.1302	
50	0.0528	-29.54	0.1301	
Ultrasound-assisted adsorption				
20	0.0331	-25.66	0.1317	12.93
30	0.0412	-27.09	0.1320	
40	0.0478	-28.37	0.1319	
50	0.0545	-29.63	0.1317	

Conclusion

Ultrasound-assisted adsorption excels at decolorization efficiency compared to the other process types owing to its lower activation energy. The lowest initial dye concentration (200 mg/L), the highest adsorbent concentration (g/L) and the highest temperature (50 °C) yielded the highest decolorization efficiency (93.3 %). Reaction time, its interaction with adsorption and its quadratic and cubic terms were retained in all the best-fit MNLR models as the most significant predictors in accounting for variation in decolorization efficiency. For future studies, the experimentally designed application of ultrasound-assisted adsorption to dye wastewaters remains to be explored in terms of economic feasibility and environmental toxicity.

ACKNOWLEDGEMENTS

The authors thank Dr. G.A. Evrendilek for her help with laboratory analysis under her supervision of YENIGIDAM project financially supported by the Turkish State Planning Organization (DPT2009K120410).

REFERENCES

1. E. Sayan and M. Esraedecan, *Ultrason. Sonochem.*, **15**, 530 (2008).
2. O. Hamdaoui, M. Chiha and E. Naffrechoux, *Ultrason. Sonochem.*, **15**, 799 (2008).
3. M.S. Tanyildizi, *Chem. Eng. J.*, **168**, 1234 (2011).
4. E. Sayan, *Chem. Eng. J.*, **119**, 175 (2006).
5. A.R. Dincer, Y. Gunes, N. Karakaya and E. Gunes, *Bioresour. Technol.*, **98**, 834 (2007).

6. S.S. Yang, W.Q. Guo, X.J. Zhou, Z.H. Meng, B. Liu and N.Q. Ren, *Bioresour. Technol.*, **102**, 9843 (2011).
7. S. Song, J. Fan, Z. He, L. Zhan, Z. Liu, J. Chen and X. Xu, *Electrochim. Acta*, **55**, 3606 (2010).
8. S. Sahinkaya, *J. Ind. Eng. Chem.*, **19**, 601 (2013).
9. A.T. Onat, T.H. Gumusdere, A. Guvenc, G. Donmez and U. Mehmetoglu, *Desalination*, **255**, 154 (2010).
10. A. Ozer and G. Dursun, *J. Hazard. Mater.*, **146**, 262 (2007).
11. O. Gulnaz, A. Kaya and S. Dincer, *J. Hazard. Mater.*, **134**, 190 (2006).
12. D. Özer, G. Dursun and A. Özer, *J. Hazard. Mater.*, **144**, 171 (2007).
13. O. Hamdaoui, *Chem. Eng. Process.*, **48**, 1157 (2009).
14. A.S. Yargic, R.Z. Yarbay Sahin, N. Özbay and E. Önal, *J. Clean. Prod.*, **88**, 152 (2015).
15. O. Lacin, B. Bayrak, O. Korkut and E. Sayan, *J. Colloid Interf. Sci.*, **292**, 330 (2005).
16. W. Nitayaphat and T. Jintakosol, *J. Clean. Prod.*, **87**, 850 (2015).
17. X.J. Zhou, W.Q. Guo, S.S. Yang and N.Q. Ren, *Bioresour. Technol.*, **105**, 40 (2012).
18. X.J. Zhou, W.Q. Guo, S.S. Yang, H.S. Zheng and N.Q. Ren, *Bioresour. Technol.*, **128**, 827 (2013).
19. T. Robinson, G. Mcmullan, R. Marchant and P. Nigam, *Bioresour. Technol.*, **77**, 247 (2001).
20. B.D. Voncina and A. Majcen-Le-Marechal, *Dyes Pigments*, **59**, 173 (2003).
21. E. Demirbas, M. Kobya and M.T. Sulak, *Bioresour. Technol.*, **99**, 5368 (2008).
22. Y. Li, W.P. Hsieh, R. Mahmudov, X. Wei and C.P. Huang, *J. Hazard. Mater.*, **244–245**, 403 (2013).
23. M.A. Behnajady, N. Modirshahla, M. Shokri and B. Vahid, *Ultrason. Sonochem.*, **15**, 1009 (2008).
24. O. Korkut, E. Sayan, O. Lacin and B. Bayrak, *Desalination*, **259**, 243 (2010).
25. W.Q. Guo, J. Ding, G.L. Cao, N.Q. Ren and F.Y. Cui, *Int. J. Hydrogen Energy*, **36**, 14180 (2011).
26. M.S. Chiou and H.Y. Li, *J. Hazard. Mater.*, **93**, 233 (2002).
27. H. Zhang, L. Duan and D. Zhang, *J. Hazard. Mater.*, **138**, 53 (2006).
28. S. Dutta, *Desalination Water Treat.*, **51**, 7631 (2013).
29. A.Y. Dursun and O. Tepe, *J. Hazard. Mater.*, **194**, 303 (2011).
30. C.H. Wu and C.H. Yu, *J. Hazard. Mater.*, **169**, 1179 (2009).
31. A. Jumasiah, T.G. Chuah, J. Gimbon, T.S.Y. Choong and I. Azni, *Desalination*, **186**, 57 (2005).
32. M. Al-Ghouti, M.A.M. Khraisheh, M.N.M. Ahmad and S. Allen, *J. Colloid Interf. Sci.*, **287**, 6 (2005).
33. M. Ozacar and I.A. Sengil, *J. Hazard. Mater.*, **98**, 211 (2003).
34. R. Gong, Y. Ding, M. Li, C. Yang, H. Liu and Y. Sun, *Dyes Pigments*, **64**, 187 (2005).
35. M. Arami, N.Y. Limaee, N.M. Mahmoodi and N.S. Tabrizi, *J. Hazard. Mater.*, **135**, 171 (2006).
36. Z. Ren, Y. Zeng and G. Zhang, *Desalination Water Treat.*, **52**, 2695 (2014).
37. A.E. Ofomaja and Y.S. Ho, *Bioresour. Technol.*, **99**, 5411 (2008).
38. A. Mittal, *J. Hazard. Mater.*, **133**, 196 (2006).